A MINI-STATE TRANSITION IN CYGNUS X-1

J. Malzac[1], P.O. Petrucci[2], E. Jourdain[1], M. Cadolle[3,4], P. Sizun[3], G. Pooley[5], C. Cabanac[2], S. Chaty[6], T. Belloni[7], J. Rodriguez[6], J.P. Roques[1], P. Durouchoux[6], A. Goldwurm[3,4], and P. Laurent[3,4]

[1]*Centre d'Etude Spatiale des Rayonnements, (CNRS/OMP/UPS), 31028 Toulouse, France*
[2]*Laboratoire d'Astrophysique Observatoire de Grenoble, BP 53 F-38041 GRENOBLE Cédex 9, France*
[3]*Service d'Astrophysique, DSM/DAPNIA/SAp, CEA-Saclay, Bat. 709, L'Orme des Merisiers, F-91 191 Gif-sur-Yvette, Cedex, France*
[4]*APC-UMR 7164, 11 place M. Berthelot, 75231 Paris, France*
[5]*Cavendish Laboratory, University of Cambridge, Madingley Road, Cambridge CB3 0HE, UK*
[6]*AIM - Astrophysique Interactions Multi-échelles (UMR 7158 CEA/CNRS/Université Paris 7 Denis Diderot), CEA Saclay, DSM/DAPNIA/Service d'Astrophysique, Bât. 709, L'Orme des Merisiers, FR-91 191 Gif-sur-Yvette Cedex, France*
[7]*INAF - Osservatorio Astronomico di Brera, via E. Bianchi 46, 23807 Merate, Italy*

ABSTRACT

We present the results of an INTEGRAL observation of Cygnus X-1 in an intermediate state. During our 4 days long observation, the source exhibited a strong flux and spectral variability correlated with the radio emission. The study of this broad band variability suggests that the source made a mini-state transition from a nearly hard state to a nearly soft state, and back.

Key words: Gamma-rays: observations –Black hole physics – Radiation mechanisms: non-thermal –X-rays: binaries; radio continuum: stars – X-rays: individual: Cygnus X-1.

1. INTRODUCTION

Cygnus X-1 is the prototype of black hole candidates. Since its discovery in 1964 (Bowyer et al. [2]), it has been intensively observed by all the high-energy instruments, from soft X-rays to γ-rays. It is a persistent source most often observed in the so-called Low Hard State (hereafter LHS), characterised by a relatively low flux in the soft X-rays ($\sim$ 1 keV) and a high flux in the hard X-rays ($\sim$ 100 keV). In the LHS, the high-energy spectrum can be roughly described by a power-law with spectral index Γ varying in the range 1.4-2.2, and a nearly exponential cut-off at a characteristic energy $E_{\rm c}$ of a few hundred keV (see e.g. Gierliǹski et al. [8]). Occasionally, the source switches to the High Soft State (HSS). The high-energy power-law is then much softer ($\Gamma > 2.4$) and the bolometric luminosity is dominated by a thermal component peaking at a few keV. Finally, there are also Intermediate States (hereafter IMS) in which the source exhibits a relatively soft X-ray spectrum ($\Gamma \sim 2.1 - 2.3$) and a moderately strong soft thermal component (Belloni et al. [1]; Mendez & van der Klis [13]). The IMS often, but not always, appears when the source is about to switch from one state to the other. When it is not associated with a state transition, it is interpreted as a 'failed state transition'.

Simultaneous radio/X-ray and high-energy observations of Cygnus X-1 and other sources have shown that the X-ray LHS is correlated with a strong radio emission which is consistent with arising from a jet (Fender [6]). In contrast, during HSS episodes the source appears to be radio weak (Brocksopp et al. [3]). The presence of a compact jet in the LHS was confirmed by Stirling et al. [14] who presented evidence for an extended and collimated radio structure on milliarsecond scales. In this paper we summarize the results of the first INTEGRAL observation of Cygnus X-1 in the open time programme (Malzac et al. [11]). This 300 ks observation was performed on 2003 June 7-11 (rev 79/80) with a 5×5 dithering pattern. At this epoch, the *RXTE* All Sky Monitor count rate of Cyg X-1 was higher than in typical LHS by up to a factor of 4, and the light curve showed strong X-ray activity characteristic of state (or failed state) transitions. We also combine the *INTEGRAL* data with the results of coordinated radio observations (15 GHz) performed with the Ryle telescope.

2. RESULTS

Fig. 1 shows the joint *JEM-X*/*ISGRI*/*SPI* spectrum fitted with a thermal/non-thermal hybrid Comptonisation model (EQPAIR model (Coppi [5]; Gierliǹski et al [9], hereafter G99; Zdziarski et al. [15], [16]) with mono energetic injection of non-thermal electrons. The unabsorbed best fit model spectrum is shown on Fig. 5. The apearence of the spectrum confirm that the source was in

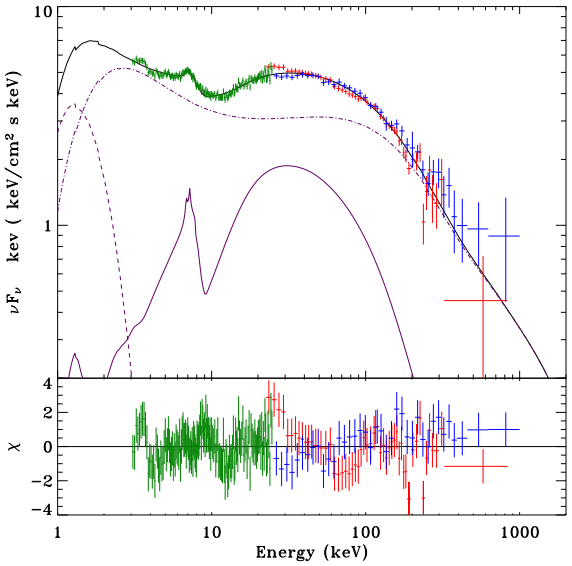

Figure 1. Joint JEM-X/SPI/ISGRI spectrum of Cygnus X-1 averaged over revolutions 79 and 80. The data are fitted with the thermal/non-thermal hybrid Comptonisation model EQPAIR *with* mono-energetic *injection of relativistic electrons. The lighter curves show the reflection component (solid), the disc thermal emission (dashed) and the Comptonised emission (dot-dashed). The green, red and blue crosses show the JEM-X, IBIS/ISGRI and SPI data respectively The temperature of the inner disk (*DISKPN*) was fixed to $kT_{\rm max}$=0.3 keV in all fits. The soft photon compactness is fixed at $l_{\rm s} = 10$. The absorbing column density is $N_{\rm h} = 5 \times 10^{21}$ and the inclination angle 45^o. The resulting best fit parameters (see G99) are the following : hard to soft compactness ratio $l_{\rm h}/l_{\rm s}$=$0.85^{+0.02}_{-0.03}$, non-thermal to hard compactness ratio $l_{\rm nth}/l_h$=$0.51^{+0.04}_{-0.04}$, electron optical depth $\tau_{\rm p}$=$0.55^{+0.01}_{-0.06}$, injection Lorentz factor $\gamma_{\rm inj}$=$8.41^{+0.62}_{-0.92}$, reflection amplitude $\Omega/2\pi = 0.71^{+0.09}_{-0.03}$, reflection ionization parameter ξ=525^{+143}_{-84} (erg cm s^{-1}), iron line energy and equivalent width $E_{\rm line}$=$7.02^{+0.32}_{-0.23}$ keV, EW= 90^{+38}_{-24} eV.*

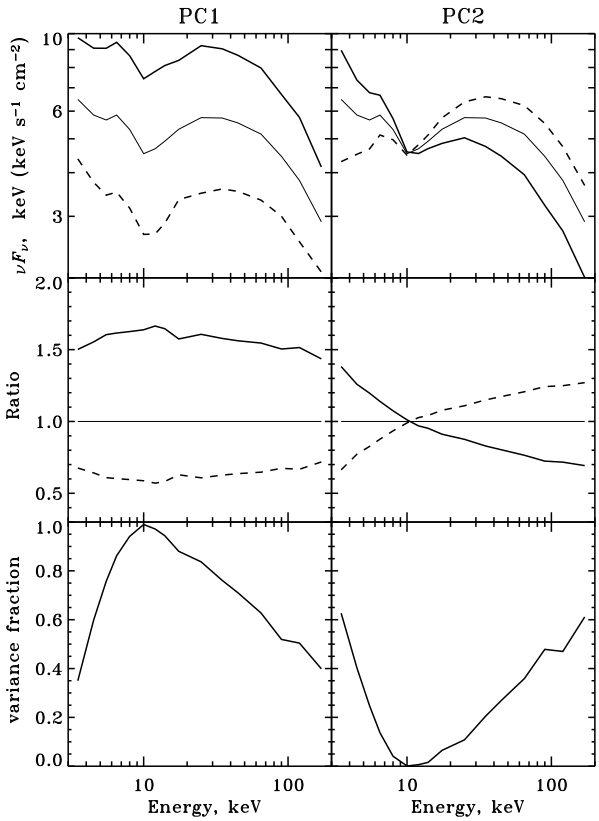

Figure 2. The 2 principal components of variability. The upper panels illustrate the effects of each component on the shape and normalisation of the spectrum: time average spectrum (light line) and spectra obtained for the maximum and minimum observed values of the normalisation parameter. The middle panels show the ratio of spectra obtained for the maximum and minimum normalisation to the average one. The bottom panels show the contribution of each component to the total variance as a function of energy.

an IMS. Moreover, the resulting best fit parameters are intermediate between what is found in the LHS and HSS. In order to study the spectral variability of the source during the observation, we produced light curves in 16 energy bands ranging from 3 to 200 keV with a time resolution of the duration of a science window (i.e. $\sim$ 30 min). The light curves exhibit a complex and strong broad band variability of the spectra as well as the overall flux. During the 4 day long observation the broad band (3–200 keV) luminosity varied by up to a factor of 2.6 and the source showed an important spectral variability. A principal component analysis demonstrates that most of this variability occurs through 2 independent modes shown in Fig. 2 and 3. The first mode (hereafter PC 1) consists in changes in the overall luminosity on time scale of hours with almost constant spectra (responsible for 68 % of the variance) We interpret this variability mode as variations of the dissipation rate in the corona, possibly associated with magnetic flares. The second variability mode (hereafter PC2) consists in a pivoting of the spectrum around $\sim$10 keV (27 % of the variance). The two spectra obtained for the minimum and maximum values of α_2 parameter controlling the amplitude of PC 2 are reminiscent of the canonical LHS and HSS spectra. PC 2 acts on a longer time-scale: initially soft, the spectrum hardens in the first part of the observation and then softens again (see Fig. 3). This pivoting pattern is strongly correlated with the radio (15 GHz) emission: radio fluxes are stronger when the *INTEGRAL* spectrum is harder (see Fig. 3 and 4) On the other hand, there is no hint of a correlation with the flaring mode as can be seen in the left panel of Fig. 4. In other terms, the radio emission is strongly correlated with the hardness and apparently unrelated to 2 to 200 keV luminosity.

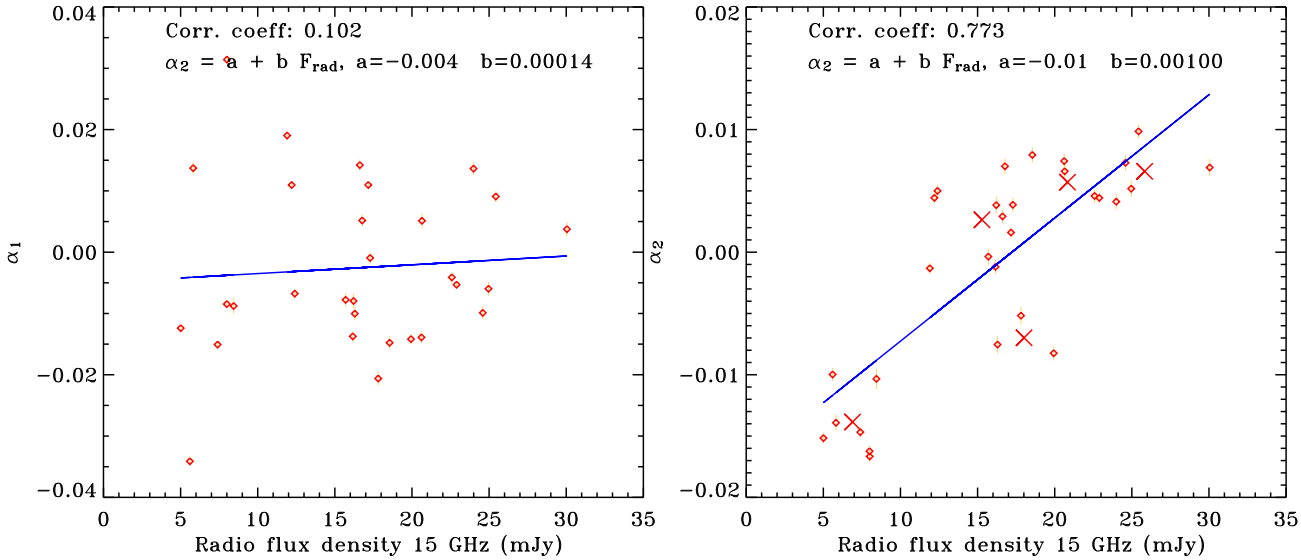

Figure 4. The amplitude of PC 1, α_1 (tracer of the luminosity, left panel) and PC 2, α_2 (tracer of the hardness, right panel) as a function of the radio flux (diamonds). In both panels, the best linear fits are shown by the solid lines. The crosses indicate the time average over each of the five periods of nearly continuous radio coverage (see Fig 3). While there is no convincing correlation between the radio flux and α_1, the radio flux is correlated to α_2 at highly significant level.

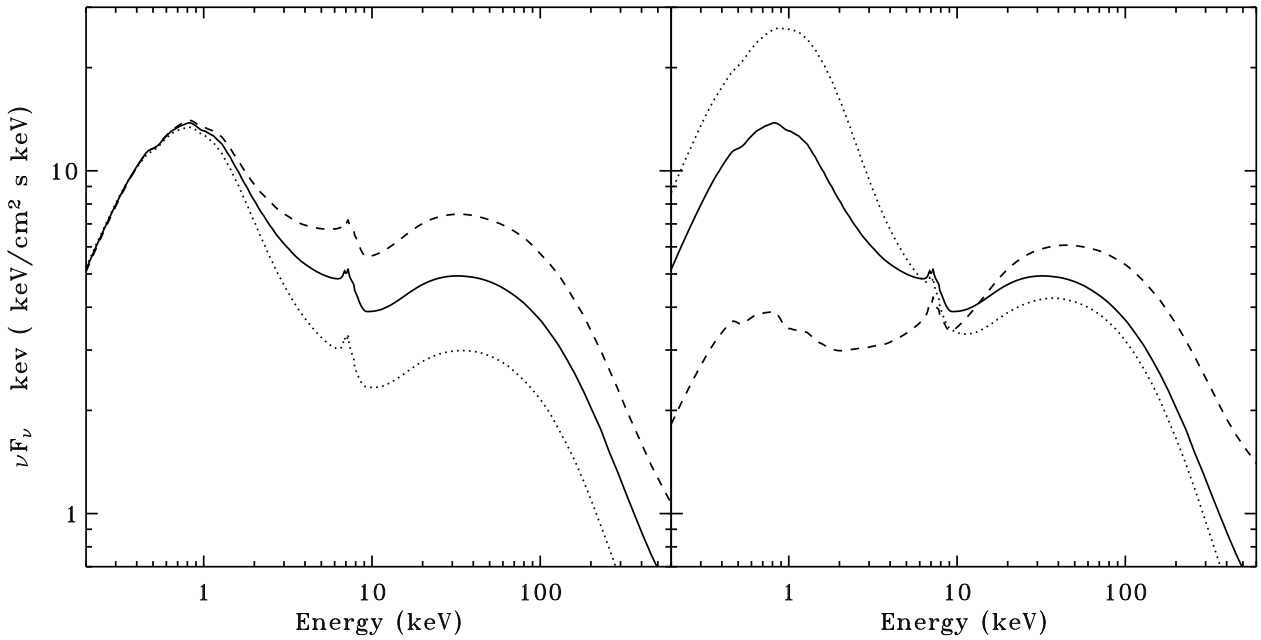

Figure 5. Left panel: effect of varying l_h by a factor of 2 on the EQPAIR *model with monoenergetic injection (see Sect. 2). Solid curve: unabsorbed best-fit model ($l_h = 8.5$); Dotted curve $l_h = 5.7$; Dashed curve: $l_h = 11.9$. Right panel: effect of varying the soft photons flux by a factor of 8. Solid curve: unabsorbed best-fit model ($T_{\rm disc} = 0.3$ keV; $l_{\rm h}/l_{\rm s} = 0.85$). Dotted curve: $T_{\rm disc} = 0.357$ keV and $l_{\rm h}/l_{\rm s} = 0.42$. Dashed curve: $T_{\rm disc} = 0.212$ keV and $l_{\rm h}/l_{\rm s} = 3.4$.*

3. DISCUSSION

We propose that the pivoting mode represents a 'mini' state transition from a nearly High Soft State to a nearly Low Hard State, and back. Actually, the transition from LHS to HSS is known to be associated with a quenching of the radio emission (Corbel et al. [4]; Gallo, Fender & Pooley [7]). As the transition to the HSS also corresponds to a strong softening of the spectrum, this is consistent with the correlation between hardness and radio flux: when, during the observation, the source gets closer to the HSS the spectrum softens and simultaneously the radio flux decreases. Moreover, compilations of LHS and

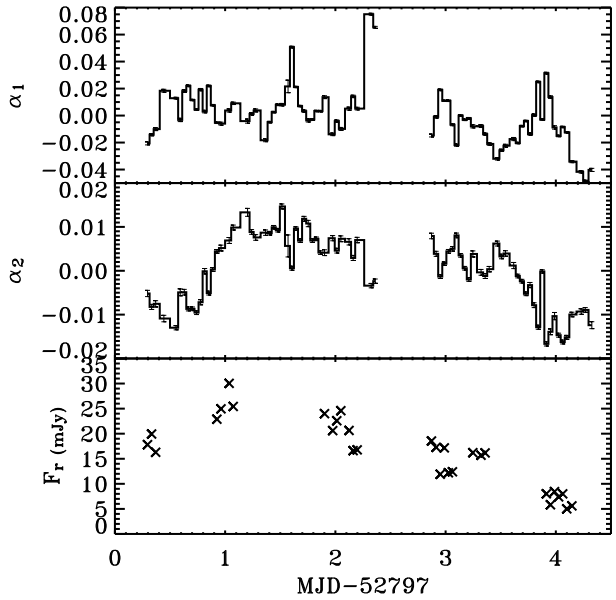

Figure 3. Evolution of α_1, the amplitude of PC 1, tracer of the luminosity (top), , α_2 , amplitude of PC 2, tracer of the hardness (middle), and radio light curve (bottom) during the observation

HSS spectra suggest that the spectral transition between LHS and HSS occurs through a pivoting around 10 keV (see e.g. Fig. 9 of McConnell et al. [12]).

It is interesting to speculate on the cause of the two variability modes. We tried to reproduce such variability modes by varying the parameters of the hybrid thermal/non-thermal Comptonisation models shown in Fig. 1. As shown in the left panel of Fig. 5 it is possible to produce variations in luminosity by a factor comparable to what is observed and little spectral changes in the *INTEGRAL* band by varying the coronal compactness $l_{\rm h}$ by a factor of 2. In this context the flaring mode would correspond to variations of the dissipation rate in the corona possibly due to magnetic reconnection. This variability mode seems to be a characteristic of the HSS (Zdziarski et al. [14]). As we show here, it also provides a major contribution to the variability of the IMS. Regarding the pivoting mode, it can be produced by changes in the flux of soft cooling photons at constant dissipation in the hot phase. We performed simulations assuming that the accretion disc radiates like a blackbody i.e. its flux $F_{disc} \propto l_{\rm s} \propto T_{\rm max}^4$ and constant l_h. For an increase of the disc temperature by a factor of 1.7, the disc luminosity grows by a factor of 8. As in this model, the disc flux also corresponds to the soft cooling photon input in the corona and the heating ($\propto l_{\rm h}$) is kept constant, this leads to a steepening of the spectrum with a pivot around 10 keV of similar amplitude as in PC 2 (see Fig. 5). For the 1996 HSS, G99 found a ratio $l_h/l_s \sim 0.3$ while in the LHS, l_h/l_s ranges between 3.5 to 15 (Ibragimov et al. [10]). The range of l_h/l_s (0.4–3.4) required to reproduce the observed amplitude of the pivoting mode matches almost exactly the intermediate range between the HSS and the lower limit of the LHS. The source initially in a (quasi) HSS evolved toward the LHS but as soon as it was reached, it went back toward the HSS. The radio versus X-ray hardness correlation would then suggest that the jet power is anti-correlated with the disc luminosity and unrelated to the coronal power. The overall change in bolometric luminosity occuring during the PC2 transition estimated from the fiducial 'hard' and 'soft' state models shown on the left panel of Fig. 5, is about a factor of 2. Because of the relatively short time scale ($\sim$ a day) on which the variation in luminosity occurs, it is unlikely to be driven by changes in the mass accretion rate. Most probably, it is due to a change in the radiative efficiency of the flow. The accretion flow could be less efficient in the LHS, because about half of the accretion power is either swallowed by the black hole or pumped into the jet, while, in the HSS, the cold disc is expected to be radiatively efficient.

ACKNOWLEDGMENTS

This paper is based on observations with *INTEGRAL*, an ESA project with instruments and science data centre funded by ESA member states (especially the PI countries: Denmark, France, Germany, Italy, Switzerland, Spain), Czech Republic and Poland, and with the participation of Russia and the USA. The Ryle Telescope is supported by PPARC.

REFERENCES

[1] Belloni, T., Mendez, M., van der Klis, M., et al., 1996, ApJ, 472, L107

[2] Bowyer, S., Byram, E.T., Chubb, T.A., Friedman, M., 1965, Sci, 147, 394

[3] Brocksopp, C., Fender, R. P., Larionov, V., Lyuty, V. M., Tarasov, A. E., Pooley, G. G., Paciesas, W. S., & Roche, P. 1999, MNRAS, 309, 1063

[4] Corbel, S., et al., 2000, A&A, 359, 251

[5] Coppi, P. S. 1999, ASP Conf. Ser. 161: High Energy Processes in Accreting Black Holes, 161, 375

[6] Fender, R. P. 2001, MNRAS, 322, 31

[7] Gallo, E., Fender, R. P., & Pooley, G. G. 2003, MNRAS, 344, 60

[8] Gierliński, M., et al., 1997, MNRAS, 288, 958

[9] Gierliński, et al. 1999, MNRAS, 309, 496 (G99)

[10] Ibragimov, A., Poutanen, J., Gilfanov, M., Zdziarski, A. A., & Shrader, C. R. 2005, MNRAS, 362, 1435

[11] Malzac, J., et al. 2006, A&A, 448, 1125

[12] McConnell, M. L., et al. 2002, ApJl, 572, 984

[13] Mendez, M. & van der Klis, M. 1997, ApJ, 479, 926

[14] Stirling, A. M., et al. 2001, MNRAS, 327, 1273

[15] Zdziarski, A. A., Poutanen, J., Paciesas, W. S., & Wen, L. 2002, ApJ, 578, 357

[16] Zdziarski, A. A., et al. 2004, MNRAS, 351, 791